PHYSICAL REVIEW D **82,** 124006 (2010)

Chameleon dark energy models with characteristic signatures

Radouane Gannouji,[1,2] Bruno Moraes,[3] David F. Mota,[4] David Polarski,[3] Shinji Tsujikawa,[2] and Hans A. Winther[4]

[1]*IUCAA, Post Bag 4, Ganeshkhind, Pune 411 007, India*

[2]*Department of Physics, Faculty of Science, Tokyo University of Science, 1-3, Kagurazaka, Shinjuku-ku, Tokyo 162-8601, Japan*

[3]*Laboratoire de Physique Théorique et Astroparticules, CNRS Université Montpellier II, France*

[4]*Institute of Theoretical Astrophysics University of Oslo, Norway*

(Received 18 October 2010; published 2 December 2010)

In chameleon dark energy models, local gravity constraints tend to rule out parameters in which observable cosmological signatures can be found. We study viable chameleon potentials consistent with a number of recent observational and experimental bounds. A novel chameleon field potential, motivated by $f(R)$ gravity, is constructed where observable cosmological signatures are present both at the background evolution and in the growth rate of the perturbations. We study the evolution of matter density perturbations on low redshifts for this potential and show that the growth index today γ_0 can have significant dispersion on scales relevant for large scale structures. The values of γ_0 can be even smaller than 0.2 with large variations of γ on very low redshifts for the model parameters constrained by local gravity tests. This gives a possibility to clearly distinguish these chameleon models from the Λ-cold-dark-matter (ΛCDM) model in future high-precision observations.

DOI: 10.1103/PhysRevD.82.124006 PACS numbers: 04.50.Kd, 95.36.+x

I. INTRODUCTION

The accelerated expansion of the Universe today is a very important challenge faced by cosmologists [1]. For an isotropic comoving perfect fluid, a substantially negative pressure is required to give rise to the cosmic acceleration. One of the simplest candidates for dark energy is the cosmological constant with an equation of state $w_{\rm DE} = -1$, but we generally encounter a problem to explain its tiny energy density consistent with observations [2].

There are alternative models of dark energy to the cosmological constant scenario. One such model is quintessence based on a minimally coupled scalar field with a self-interacting potential [3]. In order to realize the cosmic acceleration today, the mass of quintessence is required to be very small ($m_\phi \approx 10^{-33}$ GeV). From a viewpoint of particle physics, such a light scalar field may mediate a long-range force with standard model particles [4]. For example, the string dilaton can lead to the violation of the equivalence principle through the coupling with baryons [5]. In such cases we need to find some mechanism to suppress the fifth force for the consistency with local gravity experiments.

There are several different ways to screen the field interaction with baryons. One is the so-called run away dilaton scenario [6] in which the field coupling $F(\phi)$ with the Ricci scalar R is assumed to approach a constant value as the dilaton ϕ grows in time [e.g., $F(\phi) = C_1 + C_2 e^{-\phi}$ as $\phi \to \infty$]. Another way is to consider a field potential having a large mass in the region of high density where local gravity experiments are carried out. In this case the field does not propagate freely in the local region, while on cosmological scales the field mass can be light enough to be responsible for dark energy.

The latter scenario is called the chameleon mechanism in which a density-dependent matter coupling with the field can allow the possibility to suppress an effective coupling between matter and the field outside a spherically symmetric body [7,8]. The chameleon mechanism can be applied to some scalar-tensor theories such as $f(R)$ gravity [9,10] and the Brans-Dicke theory [11]. In $f(R)$ gravity, for example, there have been a number of viable dark energy models [12] that can satisfy both cosmological and local gravity constraints. For such models the potential of an effective scalar degree of freedom (called "scalaron" [13]) in the Einstein frame is designed to have a large mass in the region of high density. Even with a strong coupling between the scalaron and the baryons ($Q = -1/\sqrt{6}$), the chameleon mechanism allows the $f(R)$ models to be consistent with local gravity constraints.

The chameleon models are a kind of coupled quintessence models [14] defined in the Einstein frame [7,8]. While the gravitational action is described by the usual Einstein-Hilbert action, nonrelativistic matter components are coupled to the Einstein frame metric multiplied by some conformal factor which depends on a scalar (chameleon) field. This is how the gravitational force felt by matter is modified. While there have been many studies for experimental and observational aspects of the chameleon models [15–38], it is not clear which chameleon potentials are viable if the same field is to be responsible for dark energy.

In this paper we identify a number of chameleon potentials that can be consistent with dark energy as well as local gravity experiments. We then constrain the viable model parameter space by using the recent experimental and observational bounds—such as the 2006 Eöt-Wash experiment [39], the lunar laser ranging experiment [40], and the WMAP constraint on the time variation of particle masses

 © 2010 The American Physical Society

[41]. This can actually rule out some of the chameleon potentials with natural model parameters for the matter-coupling Q of the order of unity.

In order to distinguish the viable chameleon dark energy models from the ΛCDM model, it is crucial to study both the modifications in the evolution of the background cosmology and the modified evolution of the cosmological density perturbations. For the former, we shall consider the evolution of the so-called statefinders introduced in Refs. [42,43] and show that these parameters can exhibit a peculiar behavior different from those in the ΛCDM model.

On the other hand, the growth "index" γ of matter perturbations δ_m defined through $d\ln\delta_m/d\ln a = (\Omega_m^*)^\gamma$, where a is a scale factor and Ω_m^* is the density parameter of nonrelativistic matter, is an important quantity that allows us to discriminate between different dark energy models and interest in this quantity was revived in the context of dark energy models [44,45].

Its main importance for the study of dark energy models stems from the fact that for ΛCDM the quantity γ is known to be nearly constant with respect to the redshift z; i.e., $\gamma_{\Lambda\mathrm{CDM}} = \gamma_0 - 0.02z$ to exquisite accuracy [46], with $\gamma_0 \equiv \gamma(z=0) \approx 0.555$ [44]. As emphasized in Ref. [46], large variations of γ on low redshifts could signal that we are dealing with a dark energy model outside general relativity. This was indeed found for some scalar-tensor dark energy models [47] and $f(R)$ models [48–50]. Such large variations can also occur in models where dark energy interacts with matter [51,52]. This is exactly the case in chameleon models, which we investigate in this paper, because of the direct coupling between the chameleon field ϕ and all dustlike matter. This direct coupling is however not confined to the dark sector as in standard coupled quintessence.

An additional important point is the possible appearance of a scale dependence or dispersion in γ. Hence the behavior of γ on low redshifts can be both time-dependent and scale-dependent [53–55]. This dispersion can also be present in the models investigated here. Using the observations of large scale structure and weak lensing surveys, one can hope to detect such peculiar behaviors of γ (see, e.g., Ref. [56]). If this is the case this would signal that the gravitational law may be modified on scales relevant to large scale structures [45,54,55,57–62].

In this paper we study the evolution of γ as well as its dispersion, its dependence on the wave numbers of perturbations. We shall show that some of the chameleon models investigated here can be clearly distinguished from ΛCDM through the behavior of γ exhibiting both large variations and significant dispersion, with the possibility to obtain small values of γ today as low as $\gamma_0 \lesssim 0.2$.

II. CHAMELEON COSMOLOGY

A. Background equations

In this section we review the basic background evolution of chameleon cosmology. We consider the chameleon theory described by the following action [7,8,63]:

$$\mathcal{S} = \int d^4x\sqrt{-g}\left[\frac{R}{16\pi G} - \frac{1}{2}g^{\mu\nu}\partial_\mu\phi\partial_\nu\phi - V(\phi)\right] + \mathcal{S}_m[\Psi_m; A^2(\phi)g_{\mu\nu}], \tag{1}$$

where g is the determinant of the (Einstein frame) metric $g_{\mu\nu}$, R is the Ricci scalar, G is the bare gravitational constant, ϕ is a scalar field with a potential $V(\phi)$, and $\mathcal{S}_m$ is the matter action with matter fields Ψ_m. At low redshifts it is sufficient to consider only nonrelativistic matter (cold dark matter and baryons), but for a general dynamical analysis including high redshifts radiation must be included.

We assume that nonrelativistic matter is universally coupled to the (Jordan frame) metric $A^2(\phi)g_{\mu\nu}$, the Einstein frame metric $g_{\mu\nu}$ multiplied by a field-dependent (conformal) factor $A^2(\phi)$. This direct coupling to the field ϕ is how the gravitational interaction is modified. We can generalize this to arbitrary functions $A^{(i)}(\phi)$ for each matter component ρ_i, but in this work we will take the same function $A(\phi)$ for all components. We write the function $A(\phi)$ in the form

$$A(\phi) = e^{Q\phi/M_{\mathrm{pl}}}, \tag{2}$$

where $M_{\mathrm{pl}} = 1/\sqrt{8\pi G}$ is the reduced Planck mass and Q describes the strength of the coupling between the field ϕ and nonrelativistic matter. In the following we shall consider the case in which Q is constant. In fact, the constant coupling arises for Brans-Dicke theory by a conformal transformation to the Einstein frame [8,11]. Even when $|Q|$ is of the order of unity, it is possible to make the effective coupling between the field and matter small through the chameleon mechanism.

Let us consider the scalar field ϕ together with nonrelativistic matter (density ρ_m^*) and radiation (density ρ_r) in a spatially flat Friedmann-Lemaître-Robertson-Walker space-time with a time-dependent scale factor $a(t)$ and a metric

$$ds^2 = g_{\mu\nu}dx^\mu dx^\nu = -dt^2 + a^2(t)d\boldsymbol{x}^2. \tag{3}$$

The corresponding background equations are given by

$$3H^2 = (\rho_\phi + \rho_m^* + \rho_r)/M_{\mathrm{pl}}^2, \tag{4}$$

$$\ddot{\phi} + 3H\dot{\phi} + V_{,\phi} = -Q\rho_m^*/M_{\mathrm{pl}}, \tag{5}$$

$$\dot{\rho}_m^* + 3H\rho_m^* = Q\rho_m^*\dot{\phi}/M_{\mathrm{pl}}, \tag{6}$$

$$\dot{\rho}_r + 4H\rho_r = 0, \tag{7}$$

where $\rho_\phi \equiv \dot{\phi}^2/2 + V(\phi)$, $V_{,\phi} \equiv dV/d\phi$, and a dot represents a derivative with respect to cosmic time t. The quantity ρ_m^* is the energy density of nonrelativistic matter

in the Einstein frame and we have kept the star to avoid any confusion. Integration of Eq. (6) gives the solution $\rho_m^* \propto a^{-3}e^{Q\phi/M_{\rm pl}}$. We define the conserved matter density:

$$\rho_m \equiv e^{-Q\phi/M_{\rm pl}}\rho_m^*, \tag{8}$$

which satisfies the standard continuity equation, $\dot{\rho}_m + 3H\rho_m = 0$. Then the field equation (5) can be written in the form

$$\ddot{\phi} + 3H\dot{\phi} + V_{{\rm eff},\phi} = 0, \tag{9}$$

where $V_{\rm eff}$ is the effective potential defined by

$$V_{\rm eff} \equiv V(\phi) + e^{Q\phi/M_{\rm pl}}\rho_m. \tag{10}$$

We emphasize that it is the Einstein frame which is the physical frame. Because of the coupling between the field and matter, particle masses do evolve with time in our model.

We consider runaway positive potentials $V(\phi)$ in the region $\phi > 0$, which monotonically decrease and have a positive mass squared, i.e., $V_{,\phi} < 0$ and $V_{,\phi\phi} > 0$. We also demand the following conditions:

$$\lim_{\phi\to 0}\left|\frac{V_{,\phi}}{V}\right| = \infty, \qquad \lim_{\phi\to\infty}\frac{V_{,\phi}}{V} = 0. \tag{11}$$

The former is required to have a large mass in the region of high density, whereas we need the latter condition to realize the late-time cosmic acceleration in the region of low density. At $\phi = 0$ the potential approaches either ∞ or a finite positive value V_0. In the limit $\phi \to \infty$ we have either $V \to 0$ or $V \to V_\infty$, where V_∞ is a nonzero positive constant. If $Q > 0$ the effective potential $V_{\rm eff}(\phi)$ has a minimum at the field value $\phi_m(>0)$ satisfying the condition $V_{{\rm eff},\phi}(\phi_m) = 0$, i.e.,

$$V_{,\phi}(\phi_m) + Q(\rho_m/M_{\rm pl})e^{Q\phi_m/M_{\rm pl}} = 0. \tag{12}$$

If the potential satisfies the conditions $V_{,\phi} > 0$ and $V_{,\phi\phi} > 0$ in the region $\phi < 0$, there exists a minimum at $\phi = \phi_m(<0)$ provided that $Q < 0$. In fact this situation arises in the context of $f(R)$ dark energy models [9,10]. Since the analysis in the latter is equivalent to that in the former, we shall focus on the case $Q > 0$ and $V_{,\phi} < 0$ in the following discussion.

B. Dynamical system

In order to discuss cosmological dynamics, it is convenient to introduce the following dimensionless variables:

$$x_1 \equiv \frac{\dot{\phi}}{\sqrt{6}HM_{\rm pl}}, \qquad x_2 \equiv \frac{\sqrt{V}}{\sqrt{3}HM_{\rm pl}}, \qquad x_3 \equiv \frac{\sqrt{\rho_r}}{\sqrt{3}HM_{\rm pl}}. \tag{13}$$

Equation (4) expresses the constraint existing between these variables, i.e.,

$$\Omega_m^* \equiv \frac{\rho_m^*}{3H^2M_{\rm pl}^2} = 1 - \Omega_\phi - \Omega_r, \tag{14}$$

where

$$\Omega_\phi \equiv x_1^2 + x_2^2, \qquad \Omega_r \equiv x_3^2. \tag{15}$$

Taking the time derivative of Eq. (4) and making use of Eqs. (5)–(7), it is straightforward to derive the following equation:

$$\frac{H'}{H} = -\frac{1}{2}(3 + 3x_1^2 - 3x_2^2 + x_3^2), \tag{16}$$

where a prime represents a derivative with respect to $N \equiv \ln a$. A useful quantity is the effective equation of state

$$w_{\rm eff} = -1 - \frac{2}{3}\frac{H'}{H} = x_1^2 - x_2^2 + \frac{x_3^2}{3}. \tag{17}$$

We also introduce the field equation of state w_ϕ, as

$$w_\phi \equiv \frac{\dot{\phi}^2/2 - V(\phi)}{\dot{\phi}^2/2 + V(\phi)} = \frac{x_1^2 - x_2^2}{x_1^2 + x_2^2}. \tag{18}$$

Using Eqs. (4)–(7), we obtain the following equations:

$$x_1' = -3x_1 + \frac{\sqrt{6}}{2}\lambda x_2^2 - x_1\frac{H'}{H} - \frac{\sqrt{6}}{2}Q(1 - x_1^2 - x_2^2 - x_3^2), \tag{19}$$

$$x_2' = -\frac{\sqrt{6}}{2}\lambda x_1 x_2 - x_2\frac{H'}{H}, \tag{20}$$

$$x_3' = -2x_3 - x_3\frac{H'}{H}, \tag{21}$$

$$\lambda' = -\sqrt{6}\lambda^2(\Gamma - 1)x_1, \tag{22}$$

where

$$\lambda \equiv -\frac{M_{\rm pl}V_{,\phi}}{V}, \qquad \Gamma \equiv \frac{VV_{,\phi\phi}}{V_{,\phi}^2}. \tag{23}$$

From the conditions (11) it follows that the quantity λ decreases from ∞ to 0 as ϕ grows from 0 to ∞. Since $x_1 > 0$ in Eq. (22), the condition $\lambda' < 0$ translates into

$$\Gamma = \frac{VV_{,\phi\phi}}{V_{,\phi}^2} > 1. \tag{24}$$

Chameleon potentials shallower than the exponential potential ($\Gamma = 1$) can satisfy this condition.

Once the field settles down at the minimum of the effective potential (10), we have

$$x_1 \simeq 0, \qquad x_2 \simeq \sqrt{\frac{Q}{\lambda}\Omega_m^*}, \tag{25}$$

which gives $w_\phi \simeq -1$ from Eq. (18). As the matter density ρ_m^* decreases, the field evolves slowly along the instanta-

neous minima characterized by (25). We require that $\lambda \gg Q = \mathcal{O}(1)$ during radiation and deep matter eras for consistency with local gravity constraints in the region of high density. For the dynamical system (19)–(22) there is another fixed point called the "ϕ-matter-dominated era (ϕMDE)" [14] where $\Omega_\phi = w_{\rm eff} = 2Q^2/3$. However, since we are considering the case in which Q is of the order of unity, the effective equation of state $w_{\rm eff}$ is too large to be compatible with observations. Only when $Q < \mathcal{O}(0.1)$ the ϕMDE can be responsible for the matter era [14].

When the chameleon is slow-rolling along the minimum, we obtain the following relation from Eqs. (15) and (25):

$$\frac{\lambda}{Q} \simeq \frac{\Omega_m^*}{\Omega_\phi}. \tag{26}$$

While $\lambda \gg Q$ during the radiation and matter eras, λ becomes the same order as Q around the present epoch. The field potential is the dominant contribution on the right-hand side of Eq. (4) today, so that

$$V(\phi_0) \simeq 3H_0^2 M_{\rm pl}^2 \simeq \rho_c, \tag{27}$$

where the subscript "0" represents present values and $\rho_c \simeq 10^{-29}$ g/cm^3 is the critical density today.

III. CHAMELEON MECHANISM

In this section we review the chameleon mechanism as a way to escape local gravity constraints. In addition to the cosmological constraints discussed in the previous section, this will enable us to restrict the forms of chameleon potentials.

Let us consider a spherically symmetric space-time in the weak gravitational background with the neglect of the backreaction of metric perturbations. As in the previous section we consider the case in which couplings Q_i are the same for each matter component ($Q_i = Q$), i.e., in which the function $A(\phi)$ is given by Eq. (2). Varying the action (1) with respect to ϕ in the Minkowski background, we obtain the field equation

$$\frac{d^2\phi}{dr^2} + \frac{2}{r}\frac{d\phi}{dr} = \frac{dV_{\rm eff}}{d\phi}, \tag{28}$$

where r is the distance from the center of symmetry and $V_{\rm eff}$ is defined in Eq. (10).

Assuming that a spherically symmetric object (radius r_c and mass M_c) has a constant density $\rho_m = \rho_A$ with a homogeneous density $\rho_m = \rho_B$ outside the body, the effective potential has two minima at $\phi = \phi_A$ and $\phi = \phi_B$ satisfying the conditions

$$V_{,\phi}(\phi_A) + Q(\rho_A/M_{\rm pl})e^{Q\phi_A/M_{\rm pl}} = 0, \tag{29}$$

$$V_{,\phi}(\phi_B) + Q(\rho_B/M_{\rm pl})e^{Q\phi_B/M_{\rm pl}} = 0. \tag{30}$$

Since $Q\phi_A/M_{\rm pl} \ll 1$ and $Q\phi_B/M_{\rm pl} \ll 1$ for viable field potentials in the regions of high density, the conserved matter density ρ_m is practically indistinguishable from the matter density ρ_m^* in the Einstein frame.

The field profile inside and outside the body can be found analytically. Originally this was derived in Refs. [7,8] under the assumption that the field is frozen around $\phi = \phi_A$ in the region $0 < r < r_1$, where $r_1 (< r_c)$ is the distance at which the field begins to evolve. It is possible, even without this assumption, to derive analytic solutions by considering boundary conditions at the center of the body [26].

We consider the case in which the mass squared $m_B^2 \equiv (d^2V_{\rm eff}/d\phi^2)(\phi_B)$ outside the body satisfies the condition $m_B r_c \ll 1$, so that the m_B-dependent terms can be negligible when we match solutions at $r = r_c$. The resulting field profile outside the body ($r > r_c$) is given by [26]

$$\phi(r) = \phi_B - \frac{Q_{\rm eff}}{4\pi M_{\rm pl}}\frac{M_c}{r}, \tag{31}$$

where the effective coupling $Q_{\rm eff}$ between the field and matter is

$$Q_{\rm eff} = Q\left[1 - \frac{r_1^3}{r_c^3} + 3\frac{r_1}{r_c}\frac{1}{(m_A r_c)^2} \times \left\{\frac{m_A r_1(e^{m_A r_1} + e^{-m_A r_1})}{e^{m_A r_1} - e^{-m_A r_1}} - 1\right\}\right]. \tag{32}$$

The mass m_A is defined by $m_A^2 \equiv (d^2V_{\rm eff}/d\phi^2)(\phi_A)$. The distance r_1 is determined by the condition $m_A^2[\phi(r_1) - \phi_A] = Q\rho_A$, which translates into

$$\phi_B - \phi_A + Q\rho_A(r_1^2 - r_c^2)/(2M_{\rm pl}) = \frac{6QM_{\rm pl}\Phi_c}{(m_A r_c)^2}\frac{m_A r_1(e^{m_A r_1} + e^{-m_A r_1})}{e^{m_A r_1} - e^{-m_A r_1}}, \tag{33}$$

where $\Phi_c = M_c/(8\pi r_c) = \rho_A r_c^2/(6M_{\rm pl}^2)$ is the gravitational potential at the surface of the body.

The fifth force exerting on a test particle of a unit mass and a coupling Q is given by $\boldsymbol{F} = -Q\nabla\phi/M_{\rm pl}$. Using Eq. (31), the amplitude of the fifth force in the region $r > r_c$ is

$$F = 2|QQ_{\rm eff}|\frac{GM_c}{r^2}. \tag{34}$$

As long as $|Q_{\rm eff}| \ll 1$, it is possible to make the fifth force suppressed relative to the gravitational force GM_c/r^2. From Eq. (32) the effective coupling $Q_{\rm eff}$ can be made much smaller than Q provided that the conditions $\Delta r_c \equiv r_c - r_1 \ll r_c$ and $m_A r_c \gg 1$ are satisfied. Hence we require that the body has a thin shell and that the field is heavy inside the body for the chameleon mechanism to work.

When the body has a thin shell ($\Delta r_c \ll r_c$), one can expand Eq. (33) in terms of the small parameters $\Delta r_c/r_c$ and $1/(m_A r_c)$. This leads to

$$\epsilon_{\rm th} \equiv \frac{\phi_B - \phi_A}{6QM_{\rm pl}\Phi_c} \simeq \frac{\Delta r_c}{r_c} + \frac{1}{m_A r_c}, \tag{35}$$

where $\epsilon_{\rm th}$ is called the thin-shell parameter. As long as $m_A r_c \gg (\Delta r_c/r_c)^{-1}$, this recovers the relation $\epsilon_{\rm th} \simeq \Delta r_c/r_c$ [7,8]. The effective coupling (32) is approximately given by

$$Q_{\rm eff} \simeq 3Q\epsilon_{\rm th}. \tag{36}$$

If $\epsilon_{\rm th}$ is much smaller than 1 then one has $Q_{\rm eff} \ll Q$, so that the models can be consistent with local gravity constraints.

As an example, let us consider the experimental bound that comes from the solar system tests of the equivalence principle, namely, the lunar laser ranging (LLR) experiment, using the free-fall acceleration of the Moon ($a_{\rm Moon}$) and the Earth ($a_\oplus$) toward the Sun (mass $M_\odot$) [8,10,26]. The experimental bound on the difference of two accelerations is given by

$$\frac{2|a_{\rm Moon} - a_\oplus|}{(a_{\rm Moon} + a_\oplus)} < 10^{-13}. \tag{37}$$

Under the conditions that the Earth, the Sun, and the Moon have thin shells, the field profiles outside the bodies are given as in Eq. (31) with the replacement of corresponding quantities. The acceleration induced by a fifth force with the field profile $\phi(r)$ and the effective coupling $Q_{\rm eff}$ is $a^{\rm fifth} = |Q_{\rm eff}\nabla\phi(r)/M_{\rm pl}|$. Using the thin-shell parameter $\epsilon_{{\rm th},\oplus}$ for the Earth, the accelerations $a_\oplus$ and $a_{\rm Moon}$ are [8]

$$a_\oplus \simeq \frac{GM_\odot}{r^2}\left[1 + 18Q^2\epsilon_{{\rm th},\oplus}^2\frac{\Phi_\oplus}{\Phi_\odot}\right], \tag{38}$$

$$a_{\rm Moon} \simeq \frac{GM_\odot}{r^2}\left[1 + 18Q^2\epsilon_{{\rm th},\oplus}^2\frac{\Phi_\oplus^2}{\Phi_\odot\Phi_{\rm Moon}}\right], \tag{39}$$

where $\Phi_\odot \simeq 2.1\times10^{-6}$, $\Phi_\oplus \simeq 7.0\times10^{-10}$, and $\Phi_{\rm Moon} \simeq 3.1\times10^{-11}$ are the gravitational potentials of Sun, Earth, and Moon, respectively. Then the condition (37) reads

$$\epsilon_{{\rm th},\oplus} < \frac{8.8\times10^{-7}}{Q}. \tag{40}$$

Using the value $\Phi_\oplus \simeq 7.0\times10^{-10}$, the bound (40) translates into

$$\phi_{B,\oplus} \lesssim 10^{-15}M_{\rm pl}, \tag{41}$$

where we used the condition $\phi_{B,\oplus} \gg \phi_{A,\oplus}$. For the Earth one has $\rho_A \simeq 5$ g/cm^3 (mean density of the Earth) $\gg \rho_B \simeq 10^{-24}$ g/cm^3 (dark matter/baryon density in our galaxy), so that the condition $\phi_{B,\oplus} \gg \phi_{A,\oplus}$ is satisfied.

In Sec. IV we constrain viable chameleon potentials by employing the condition (41) together with the cosmological condition we discussed in Sec. II. In Sec. V we restrict the allowed model parameter space further by using a number of recent local gravity and observational constraints.

IV. VIABLE CHAMELEON POTENTIALS

We now discuss the forms of viable field potentials that can be in principle consistent with both local gravity and cosmological constraints. Let us consider the potential

$$V(\phi) = M^4 f(\phi), \tag{42}$$

where M is a mass scale and $f(\phi)$ is a dimensionless function in terms of ϕ.

The local gravity constraint coming from the LLR experiment is given by Eq. (41), where $\phi_{B,\oplus}$ is determined by solving

$$|M_{\rm pl}f_{,\phi}(\phi_{B,\oplus})| \simeq Q\rho_B/M^4. \tag{43}$$

Here we take $\rho_B \simeq 10^{-24}$ g/cm^3 for the homogeneous density outside the Earth. Once the form of $f(\phi)$ is specified, the constraint on the model parameter, e.g., M, can be derived.

From the cosmological constraint (26), λ/Q is of the order of 1 today. Then it follows that

$$|M_{\rm pl}f_{,\phi}(\phi_0)| \simeq Qf(\phi_0) \simeq Q\rho_c/M^4, \tag{44}$$

where we used Eq. (27).

We also require the condition (24), i.e.,

$$\Gamma = \frac{ff_{,\phi\phi}}{f_{,\phi}^2} > 1, \tag{45}$$

for all positive values of ϕ. We shall proceed to find viable potentials satisfying the conditions (41) and (43)–(45). From Eqs. (43) and (44) we obtain

$$\frac{f_{,\phi}(\phi_{B,\oplus})}{f_{,\phi}(\phi_0)} \simeq \frac{\rho_B}{\rho_c} \simeq 10^5. \tag{46}$$

Let us consider the inverse-power-law potential $V(\phi) = M^{4+n}\phi^{-n}$ ($n > 0$), i.e.,

$$f(\phi) = (M/\phi)^n. \tag{47}$$

Since $\Gamma = (n+1)/n > 1$, the condition (45) is automatically satisfied. The cosmological constraint (44) gives

$$\phi_0 \simeq nM_{\rm pl}/Q. \tag{48}$$

From Eq. (46) we find the relation between ϕ_0 and $\phi_{B,\oplus}$:

$$\phi_0 \simeq 10^{5/(n+1)}\phi_{B,\oplus}. \tag{49}$$

Using the LLR bound (41), it follows that

$$\phi_0 \lesssim 10^{-5(3n+2)/(n+1)}M_{\rm pl}. \tag{50}$$

This is incompatible with the cosmological constraint (48) for $n \geq 1$ and $Q = \mathcal{O}(1)$. Hence the inverse-power-law potential is not viable.

A. Inverse-power-law potential + constant

The reason why the inverse-power-law potential does not work is that the field value today required for cosmic acceleration is of the order of $M_{\rm pl}$, while the local gravity constraint demands a much smaller value. This problem can be circumvented by taking into account a constant term to the inverse-power-law potential. Let us then consider the potential $V(\phi) = M^4[1 + \mu(M/\phi)^n]$ $(n > 0)$, i.e.,

$$f(\phi) = 1 + \mu(M/\phi)^n, \tag{51}$$

where μ is a positive constant. The rescaling of the mass term M always allows us to normalize the constant to be unity in Eq. (51). For this potential the quantity Γ reads

$$\Gamma = \frac{n+1}{n}\left[1 + \frac{1}{\mu}\left(\frac{\phi}{M}\right)^n\right], \tag{52}$$

which satisfies the condition $\Gamma > 1$. In the region $\mu(M/\phi)^n \gg 1$ we have that $\Gamma \simeq (n+1)/n$, which recovers the case of the inverse-power-law potential. Meanwhile, in the region $\mu(M/\phi)^n \ll 1$, one has $\Gamma \gg 1$. The latter property comes from the fact that the potential becomes shallower as the field ϕ increases. This modification of the potential allows a possibility that the model can be consistent with both cosmological and local gravity constraints.

The addition of a constant term to the inverse-power-law potential does not affect the condition (46), which means that the resulting bounds (49) and (50) are not subject to change. On the other hand, the cosmological constraint (48) is modified. Let us consider the case where the condition $\mu(M/\phi_0)^n \ll 1$ is satisfied today, i.e., $f(\phi_0) \simeq 1$. From Eq. (44) it follows that

$$M \simeq \rho_c^{1/4} \simeq 10^{-12}\ \text{GeV}, \tag{53}$$

and

$$\phi_0 \simeq \left(n\mu\frac{M^n}{M_{\rm pl}^n}\right)^{1/(n+1)} M_{\rm pl} \simeq (10^{-30n} n\mu)^{1/(n+1)} M_{\rm pl}. \tag{54}$$

Hence the field value ϕ_0 today can be much smaller than the Planck mass, unlike the inverse-power-law potential. From Eqs. (50) and (54) we get the constraint

$$\mu \lesssim 10^{15n-10}/n. \tag{55}$$

If $n = 1$, for example, one has $\mu \lesssim 10^5$. For larger n the bound on μ becomes even weaker. We note that the condition $\mu(M/\phi)^n < 1$ is satisfied for $\phi/M_{\rm pl} \gtrsim 10^{-10/n-15}/n^{1/n}$. This shows that even the field value such as $\phi_{B,\oplus} = 10^{-15} M_{\rm pl}$ satisfies the condition $\mu(M/\phi_{B,\oplus})^n < 1$. Thus the term $\mu(M/\phi)^n$ is smaller than 1 for the field values we are interested in ($\phi_{B,\oplus} \lesssim \phi \lesssim \phi_0$).

A large range of experimental bounds for this model has been derived in the literature (see Refs. [8,17,20,24]). For $Q = n = 1$, it was found in Ref. [20] that the model is ruled out by the Eöt-Wash experiment unless $\mu \lesssim 10^{-5}$. This applies for general n: to obtain a viable model for Q of the order of unity one must impose a fine-tuning $n \gg 1$ or $\mu \ll 1$.

The potentials, which have only one mass scale equivalent to the dark energy scale, are usually strongly constrained by the Eöt-Wash experiment. We shall look into this issue in more detail in Sec. V.

B. Construction of viable chameleon potentials relevant to dark energy

The discussion given above shows that a function $f(\phi)$ that monotonically decreases without a constant term has difficulty satisfying both cosmological and local gravity constraints. This is associated with the fact that for any power-law form of $f(\phi)$ the condition $|M_{\rm pl} f_{,\phi}(\phi_0)/f(\phi_0)| \simeq 1$ leads to the overall scaling of the function $f(\phi_0)$ itself, giving ϕ_0 of the order of $M_{\rm pl}$. The dominance of a constant term in $f(\phi_0)$ changes this situation, which allows a much smaller value of ϕ_0 relative to $M_{\rm pl}$.

Another example similar to $V(\phi) = M^4[1 + \mu(M/\phi)^n]$ is the potential [15]

$$V(\phi) = M^4 \exp[\mu(M/\phi)^n], \tag{56}$$

where $\mu > 0$ and $n > 0$. For this model the quantity

$$\Gamma = 1 + \frac{n+1}{n}\frac{1}{\mu}\left(\frac{\phi}{M}\right)^n \tag{57}$$

is larger than 1. In the asymptotic regimes characterized by $\mu(M/\phi)^n \gg 1$ and $\mu(M/\phi)^n \ll 1$ we have $\Gamma \simeq 1$ and $\Gamma \gg 1$, respectively. When $\mu(M/\phi)^n \ll 1$ the function $f(\phi) = \exp[\mu(M/\phi)^n]$ can be approximated as $f(\phi) \simeq 1 + \mu(M/\phi)^n$, which corresponds to Eq. (51). In this case the constraints on the model parameters are the same as those given in Eqs. (53)–(55).

There is another class of potentials that behaves as $V(\phi) \simeq M^4[1 - \mu(\phi/M)^n]$ $(\mu > 0,\ 0 < n < 1)$ in the region $\mu(\phi/M)^n \ll 1$. In fact this asymptotic form corresponds to the potential that appears in $f(R)$ dark energy models. While the potential is finite at $\phi = 0$ the derivative $|V_{,\phi}|$ diverges as $\phi \to 0$ for $0 < n < 1$, so that the first of the condition (11) is satisfied. In order to keep the potential positive we need some modification of V in the region $\mu(\phi/M)^n > 1$.

In scalar-tensor theory it was shown in Ref. [11] that the Jordan frame potential of the form $U(\phi) = M^4[1 - \mu(1 - e^{-2Q\phi/M_{\rm pl}})^n]$ $(0 < \mu < 1,\ 0 < n < 1)$ can satisfy both cosmological and local gravity constraints. In this case the potential $V(\phi)$ in the Einstein frame is given by $V(\phi) = e^{4Q\phi/M_{\rm pl}} U(\phi)$, which possesses a de Sitter minimum due to the presence of the conformal factor. Cosmologically the solutions finally approach the de Sitter fixed point, so that the late-time cosmic acceleration can be realized.

Now we would like to consider a runaway positive potential in the Einstein frame. One example is

$$V(\phi) = M^4[1 - \mu(1 - e^{-\phi/M_{\rm pl}})^n], \tag{58}$$

where $0 < \mu < 1$ and $0 < n < 1$. This potential behaves as $V(\phi) \simeq M^4[1 - \mu(\phi/M_{\rm pl})^n]$ for $\phi \ll M_{\rm pl}$ and approaches $V(\phi) \to M^4(1 - \mu)$ in the limit $\phi \gg M_{\rm pl}$ (see Fig. 1). For the potential (58) we obtain

$$\Gamma - 1 = \frac{1 - nx - \mu(1 - x)^n}{n\mu x(1 - x)^n}, \qquad x \equiv e^{-\phi/M_{\rm pl}}. \tag{59}$$

One can easily show that the right-hand side is positive under the conditions $0 < \mu < 1$, $0 < n < 1$, so that $\Gamma > 1$. In both limits $\phi \to 0$ and $\phi \to \infty$ one has $\Gamma \to +\infty$. Since Γ has a minimum at a finite field value, the condition $\Gamma \gg 1$ is not necessarily satisfied today [unlike the potential (56)].

Unless μ is very close to 1 the potential energy today is roughly of the order of M^4, i.e., $f(\phi_0) \approx 1$. From Eq. (44) it then follows that

$$n\mu(1 - x_0)^{n-1}x_0 \simeq Q, \tag{60}$$

where $x_0 \equiv e^{-\phi_0/M_{\rm pl}}$. If $\phi_0 \ll M_{\rm pl}$, we have that $\phi_0/M_{\rm pl} \simeq (n\mu)^{1/(1-n)}$. From Eq. (43) we obtain

$$n\mu(1 - x_B)^{n-1}x_B \simeq 10^5 Q, \tag{61}$$

where $x_B \equiv e^{-\phi_B/M_{\rm pl}}$. Under the condition $\phi_B \ll M_{\rm pl}$ we have $\phi_B/M_{\rm pl} \simeq (10^{-5}n\mu/Q)^{1/(1-n)}$ from Eq. (61). Then the LLR bound (41) corresponds to

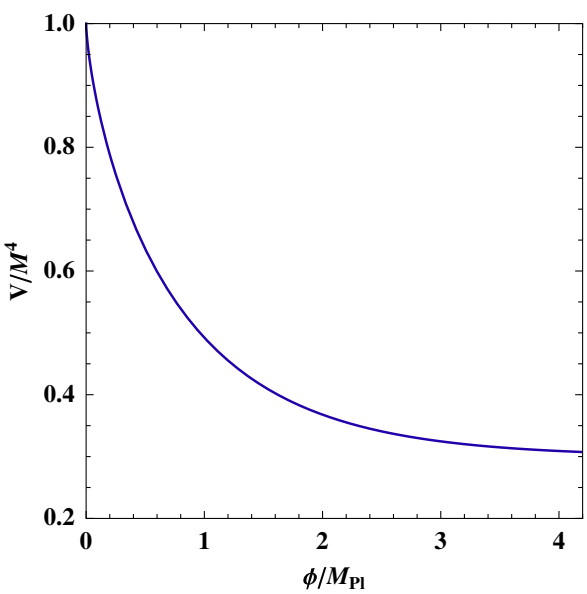

FIG. 1 (color online). The potential (58) versus the field ϕ for $\mu = 0.7$ and $n = 0.7$. The potential has a finite value $V = M^4$ at $\phi = 0$, but its derivatives diverge ($|V_{,\phi}| \to \infty$ and $V_{,\phi\phi} \to \infty$) as $\phi \to 0$.

$$n \cdot 10^{10-15n} < Q/\mu. \tag{62}$$

When $\mu = 0.5$ and $\mu = 0.05$ with $Q = 1$, the constraint (62) gives $n \gtrsim 0.63$ and $n \gtrsim 0.56$, respectively.

C. Statefinder analysis

The statefinder diagnostics introduced in Refs. [42,43] can be a useful tool to distinguish dark energy models from the ΛCDM model. The statefinder parameters are defined by

$$r = \frac{\ddot{a}}{aH^3}, \qquad s = \frac{r - 1}{3(q - 1/2)}, \tag{63}$$

where $q \equiv -\ddot{a}/(aH^2)$ is the deceleration parameter. Defining $h \equiv H^2$, it follows that

$$q = -1 - \frac{h'}{2h}, \qquad r = 1 + \frac{h''}{2h} + \frac{3h'}{2h}, \tag{64}$$

where a prime represents a derivative with respect to $N = \ln a$.

In the radiation dominated epoch we have $h \propto e^{-4N}$, which gives $(r, s) \simeq (3, 4/3)$. During the matter era r approaches 1, whereas s blows up from positive to negative because of the divergence of the denominator in s (i.e., $q = 1/2$). For the chameleon potentials (56) and (58) the solutions finally approach the de Sitter fixed point characterized by $(r, s) = (1, 0)$. Around the de Sitter point the solutions evolve along the instantaneous minima characterized by $(x_1, x_2, x_3) = (\lambda/\sqrt{6}, \sqrt{1 - \lambda^2/6}, 0)$ with $h \propto V$. Using Eq. (22) as well, one has $h'/h \simeq -\lambda^2$ and $h''/h \simeq (2\Gamma - 1)\lambda^4$. Then the statefinder diagnostics around the de Sitter point can be estimated as

$$r \simeq 1 + \left(\Gamma - \frac{1}{2}\right)\lambda^4 - \frac{3}{2}\lambda^2, \tag{65}$$

$$s \simeq -\frac{(2\Gamma - 1)\lambda^4 - 3\lambda^2}{3(3 - \lambda^2)}. \tag{66}$$

Since λ finally approaches 0, Eq. (22) implies that $\Gamma\lambda^3 \to 0$ asymptotically. For the potential in which $\Gamma \gg 1$ holds today it can happen that $\Gamma\lambda^4 \gg \lambda^2$, which gives $r \simeq 1 + \Gamma\lambda^4 > 1$ and $s \simeq -2\Gamma\lambda^4/[3(3 - \lambda^2)] < 0$ around the present epoch. In the upper panel of Fig. 2 we plot the evolution of the variables r and s for the potential (56) in the redshift regime $-1 < z \equiv 1/a - 1 < 10$. The statefinders evolve toward the de Sitter point characterized by $(r, s) = (1, 0)$ from the regime $r > 1$ and $s < 0$. This behavior is different from quintessence with the power-law potential $V(\phi) = M^{4+n}\phi^{-n}$ ($n > 0$) in which the statefinders are confined in the region $r < 1$ and $s > 0$ [42,43].

The potential (58) allows the possibility that Γ is not much larger than 1 even at the present epoch. In the regime $\lambda^2 \ll 1$ we then have $r \simeq 1 - 3\lambda^2/2 < 1$ and $s \simeq \lambda^2/3 > 0$. In fact we have numerically confirmed that the solutions

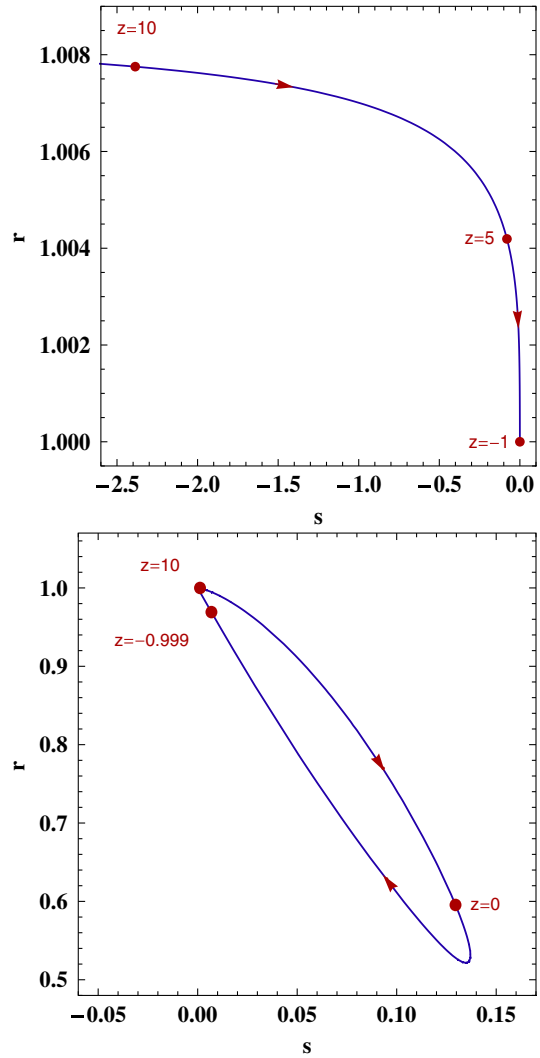

FIG. 2 (color online). (Top) Evolution of the statefinders r and s for the potential (56) with $n = 1$, $Q = 1$, and $\mu = 1$. The solutions approach the de Sitter point at $(r, s) = (1, 0)$ from the region $r > 1$ and $s < 0$. (Bottom) Evolution of statefinders for the potential (58) with $n = 0.7$, $Q = 1$, and $\mu = 0.7$. In this case the solutions approach the de Sitter point from the region $r < 1$ and $s > 0$.

enter this regime by today (see the lower panel of Fig. 2). Finally they approach the de Sitter point from the regime $r < 1$ and $s > 0$. Hence one can distinguish between chameleon potentials from the evolution of statefinders.

V. LOCAL GRAVITY CONSTRAINTS ON CHAMELEON POTENTIALS

In this section we discuss a number of local gravity constraints on the chameleon potentials (56) and (58) in details. Together with the LLR bound (41) we use the constraint coming from 2006 Eöt-Wash experiments [39] as well as the WMAP bound on the variation of the field-dependent mass.

A. The WMAP constraint on the variation of the particle mass

Because of the conformal coupling of the field ϕ to matter, any particle will acquire a ϕ-dependent mass:

$$m(\phi) = m_0 e^{Q\phi/M_{\rm pl}}, \tag{67}$$

where m_0 is a constant.

The WMAP data constrain any variation in $m(\phi)$, between now and the epoch of recombination to be $\lesssim$ 5% at 2σ ($\lesssim$ 23% at 4σ) [41]. We then require that

$$\left|\frac{\Delta m(\phi)}{m}\right| = |e^{Q(\phi_0-\phi_{\rm rec})/M_{\rm pl}} - 1| \lesssim 0.05, \tag{68}$$

where $\phi_{\rm rec}$ is the field value at the recombination epoch. If we assume that the chameleon follows the minimum since recombination then $\phi_0 \gg \phi_{\rm rec}$, and the field in the cosmological background today must satisfy

$$Q\phi_0/M_{\rm pl} \lesssim 0.05. \tag{69}$$

This provides a constraint on the coupling Q and the model parameters of chameleon potentials.

Note that the WMAP constraint is not a local gravity constraint. Nevertheless, it provides strong constraints on the potential (58) with natural parameters and is therefore considered in this section.

B. Constraints from the 2006 Eöt-Wash experiment

The 2006 Eöt-Wash experiment [39] searched for deviations from the $1/r^2$ force law of gravity. The experiment used two parallel plates, the detector and attractor, which are separated by a (smallest) distance $d = 55\mu$m. The plates have holes of different sizes bored into them, and the attractor is rotating with an angular velocity ω. The rotation of the attractor gives rise to a torque on the detector, and the setup of the experiment is such that this torque vanishes for any force that falls off as $1/r^2$. In between the plates there is a $d_s = 10\mu$m BeCu sheet, which is for shielding the detector from electrostatic forces.

The chameleon force between two parallel plates (see, e.g., Ref. [24]) usually falls off faster than $1/r^2$, implying a strong signature on the experiment. However, if the matter coupling is strong enough, the electrostatic shield will itself develop a thin shell. When this happens, the effect of this shield is not only to shield electrostatic forces, but also to shield the chameleon force on the detector. This suppression is approximately given by a factor $\exp(-m_s d_s)$, where m_s is the mass inside the electrostatic shield. Hence the experiment cannot detect strongly coupled chameleons.

The behavior of chameleons in the Eöt-Wash experiment has been explained in Refs. [20,27,38]. We calculate the Eöt-Wash constraints on our models numerically based on the prescription presented in Ref. [27].

C. Combined local gravity constraints

1. Potential $V(\phi) = M^4 \exp[\mu(M/\phi)^n]$

Let us first consider the inverse-power-law potential (56) with $n > 0$. From Eq. (12) the field value ϕ_m at the minimum of the effective potential $V_{\rm eff}$ satisfies

$$\left(\frac{M}{\phi_m}\right)^{n+1} = \frac{Q}{\mu n}\frac{M}{M_{\rm pl}}\frac{\rho_m e^{Q\phi_m/M_{\rm pl}}}{V(\phi_m)}. \tag{70}$$

In this model the field is in the regime $M \ll \phi_m \ll M_{\rm pl}$ for the density ρ_m we are interested in. Since $V(\phi_m)$ can be approximated as $V(\phi_m) \simeq M^4$, it follows that

$$\frac{\phi_m}{M} \simeq \left(\frac{Q}{\mu n}\frac{M}{M_{\rm pl}}\frac{\rho_m}{M^4}\right)^{-1/(n+1)}. \tag{71}$$

Using the LLR bound (41) with the homogeneous density $\rho_m \simeq 10^{-24}$ g/cm^3 in our galaxy, we obtain the constraint

$$n \cdot 10^{10-15n} < Q/\mu. \tag{72}$$

The WMAP bound (69) gives

$$Q < \frac{M_{\rm pl}}{M}\left(\frac{0.05^{n+1}}{\mu n}\frac{\rho_m^{(0)}}{M^4}\right)^{1/n}, \tag{73}$$

where $\rho_m^{(0)}$ is the matter density today, with $\rho_m^{(0)}/M^4 \approx \Omega_m^{*(0)}/\Omega_\phi^{(0)} \approx 1/3$. Since $M_{\rm pl}/M \approx 10^{30}$, this condition is well satisfied for Q, n, μ of the order of unity.

For the Eöt-Wash experiment, the chameleon torque on the detector was found numerically to be larger than the experimental bound when Q, n, μ are of the order of unity. Providing the electrostatic shield with a thin shell, we require that $n \gg 1$, $Q \gg 1$, or $\mu \ll 1$ to satisfy the experimental bound.

In Fig. 3 we plot the region constrained by the bounds (72) and (73), and the Eöt-Wash experiment for $\mu = 1$. This shows that only the large coupling region with $Q \gg 1$ can be allowed for n of the order of unity. A viable model can also be constructed by taking values of μ much smaller than 1. Note that the WMAP bound (73) is satisfied for the parameter regime shown in Fig. 3.

2. Potential $V(\phi) = M^4[1 - \mu(1 - e^{-\phi/M_{\rm pl}})^n]$

Let us proceed to another potential (58) with $0 < n < 1$. In the regions of high density where local gravity experiments are carried out, we have $\phi \ll M_{\rm pl}$ and hence $V(\phi) \simeq M^4[1 - \mu(\phi/M_{\rm pl})^n]$. In this regime the effective potential $V_{\rm eff}$ has a minimum at

$$\phi_m = \left(\frac{Q}{\mu n}\frac{\rho_m}{M^4}\right)^{1/(n-1)} M_{\rm pl}. \tag{74}$$

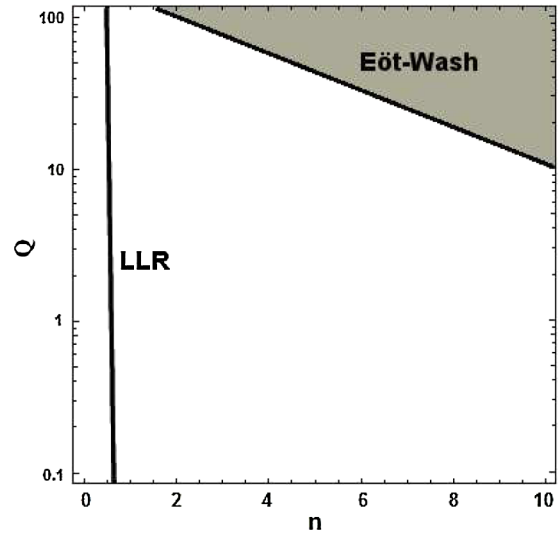

FIG. 3 (color online). The combined local gravity constraints on the potential (56) with $\mu = 1$ in the (n, Q) plane. The shaded region corresponds to the allowed parameter space. The natural values of Q and n of the order of unity are excluded.

Recall that the LLR bound was already derived in Eq. (62), which is the same as the constraint (72) of the previous potential.

Assuming that the chameleon is at the minimum of its effective potential in the cosmological background today, the WMAP bound (69) translates into

$$Q \gtrsim 0.05(60n\mu)^{1/n}, \tag{75}$$

where we have used $\rho_m^{(0)}/M^4 \approx 1/3$ in Eq. (74). However, a full numerical simulation of the background evolution shows that this is not always the case. For a large range of parameters the chameleon has started to lag behind the minimum, which again leads to a weaker constraint.

The Eöt-Wash experiment provides the strongest constraints when Q is of the order of unity for the potentials (51) and (56). This is not the case for the potential (58), because the electrostatic shield used in the experiment develops a thin shell.

The mass inside the electrostatic shield is given by

$$m_s^2 \simeq n(1-n)\mu\left(\frac{Q\rho_s}{\mu n M^4}\right)^{(2-n)/(1-n)}\frac{M^4}{M_{\rm pl}^2}. \tag{76}$$

Using $\rho_s \simeq 10$ g/cm^3 and $d_s \simeq 10\mu$m we have

$$m_s d_s \simeq \sqrt{n(1-n)\mu}\left(\frac{Q}{\mu n}\right)^{(2-n)/(1-n)} 10^{(6-35n)/(1-n)}. \tag{77}$$

Taking Q and μ to be of the order of unity, we find $m_s d_s \gg 1$ as long as $n \gtrsim 0.2$. The suppression of the chameleon torque due to the presence of the electrostatic shield makes the chameleon invisible in the experiment.

In Figs. 4 and 5 we plot the allowed regions constrained by the bounds (62) and (75), and the Eöt-Wash

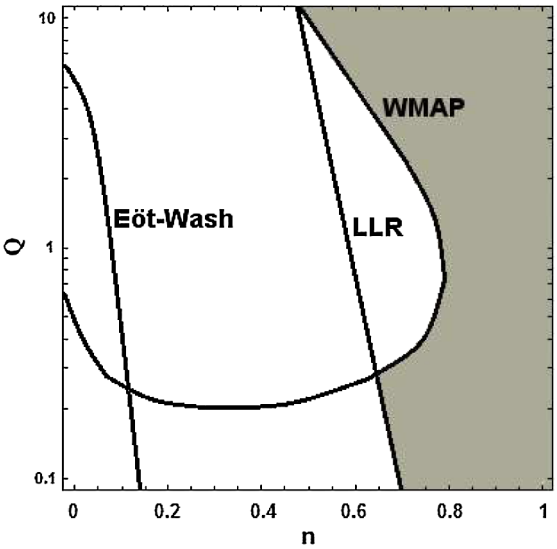

FIG. 4 (color online). The combined local gravity constraints on the potential (58) with $\mu = 0.5$ in the (n, Q) plane. In this case the allowed parameter space (shaded region in the figure) is determined by the WMAP constraint and the LLR constraint.

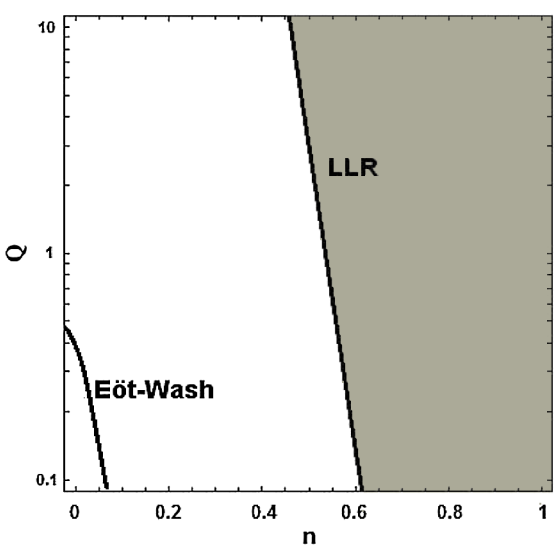

FIG. 5 (color online). The combined local gravity constraints on the potential (58) with $\mu = 0.05$. The allowed parameter space is determined by the LLR bound. The WMAP constraint is satisfied for the whole parameter space in the figure.

experiments, for $\mu = 0.5$ and $\mu = 0.05$, respectively. When $\mu = 0.5$ the WMAP constraint gives the tightest bound for $Q \gtrsim 0.2$, and the parameter space $Q \lesssim 1$ is viable for $n \gtrsim 0.7$. If we decrease the values of μ down to 0.05, then the WMAP bound is well satisfied for the parameter space shown in Fig. 5. Instead, the LLR experiment provides the tightest bound in such cases. When $\mu = 0.05$, the region with $0.1 \lesssim Q \lesssim 10$ and $n \gtrsim 0.6$ can be allowed. The coupling Q as well as the parameter n are not severely constrained for the potential (58).

VI. LINEAR GROWTH OF MATTER PERTURBATIONS

We now turn our attention to cosmological perturbations in chameleon cosmology. It is well-known that matter perturbations allow us to discriminate between dark energy models where the gravitational interaction is modified on cosmic scales. We first review the general formalism and derive the equation for linear matter perturbations. We also introduce important quantities like the critical scale λ_c below which modifications of gravity are felt and the growth index $\gamma(z, k)$, a powerful discriminative quantity for the study of the modified evolution of matter perturbations as was explained in the introduction.

As we have seen in Sec. V, local gravity constraints impose very strong boundaries on the potential (56), forcing its parameters to take unnatural values. Moreover, for viable choices of parameters, we have verified that the linear perturbations behave in a manner similar to the ΛCDM model, as λ_c is much smaller than the cosmic scales we are interested in. On the other hand we have shown that the model parameters of the potential (58) are not severely constrained. In Sec. VI B we will show that the potential (58) gives rise to some very interesting observational signatures.

A. General formalism for cosmological perturbations

We consider scalar metric perturbations α, B, ψ, and γ around a flat Friedmann-Lemaître-Robertson-Walker background. The line element describing such a perturbed Universe is given by [64]

$$ds^2 = -(1 + 2\alpha)dt^2 - 2aB_{,i}dtdx^i + a(t)^2[(1 + 2\psi)\delta_{ij} + 2\gamma_{,i;j}]dx^i dx^j. \quad (78)$$

We decompose the field ϕ into the background and inhomogeneous parts: $\phi(t, \boldsymbol{x}) = \tilde{\phi}(t) + \delta\phi(t, \boldsymbol{x})$. The energy-momentum tensors $T^{(m)}_{\mu\nu}$ of nonrelativistic matter can be decomposed as

$$T^{0(m)}_0 = -(\rho^*_m + \delta\rho^*_m), \qquad T^{0(m)}_i = -\rho^*_m v_{,i}, \quad (79)$$

where v is the peculiar velocity potential of nonrelativistic matter. In the following, when we express background quantities, we drop the tilde for simplicity.

Let us consider the evolution of matter perturbations, $\delta_m \equiv \delta\rho^*_m/\rho^*_m$ in the comoving gauge ($v = 0$). The quantity δ_m corresponds to the gauge-invariant quantity introduced in Refs. [64–66] when expressed in the comoving gauge. In the Fourier space the first-order perturbation equations are given by [67,68]

$$\alpha = -Q\delta\phi/M_{\rm pl}, \quad (80)$$

$$\delta\dot{\rho}^*_m + 3H\delta\rho^*_m - \rho^*_m(\kappa - 3H\alpha) - Q(\rho^*_m\dot{\delta\phi} + \delta\rho^*_m\dot{\phi})/M_{\rm pl} = 0, \quad (81)$$

$$\delta\ddot{\phi} + 3H\delta\dot{\phi} + \left(V_{,\phi\phi} + \frac{k^2}{a^2}\right)\delta\phi + 2\alpha V_{,\phi} - \dot{\phi}(\dot{\alpha} - 3H\alpha + \kappa) + Q(2\alpha\rho_m^* + \delta\rho_m^*)/M_{\rm pl} = 0, \quad (82)$$

$$\dot{\kappa} + 2H\kappa + 3\dot{H}\alpha - \frac{k^2}{a^2}\alpha - \frac{1}{2M_{\rm pl}^2}(\delta\rho_m^* - 4\alpha\dot{\phi}^2 + 4\dot{\phi}\,\delta\dot{\phi} - 2V_{,\phi}\delta\phi) = 0, \quad (83)$$

where k is a comoving wave number and $\kappa \equiv 3(H\alpha - \dot{\psi}) + (k^2/a)(B + a\dot{\gamma})$. From Eq. (81) it follows that

$$\kappa = \dot{\delta}_m - Q(\delta\dot{\phi} + 3H\delta\phi)/M_{\rm pl}, \quad (84)$$

where we have used Eq. (80). Plugging Eq. (84) into Eqs. (82) and (83), we obtain

$$\delta\ddot{\phi} + \left(3H + 2Q\frac{\dot{\phi}}{M_{\rm pl}}\right)\delta\dot{\phi} + \left(m_\phi^2 + \frac{k^2}{a^2} - 2Q\frac{V_{,\phi}}{M_{\rm pl}} - 2Q^2\frac{\rho_m^*}{M_{\rm pl}^2}\right)\delta\phi + \frac{Q}{M_{\rm pl}}\rho_m^*\delta_m - \dot{\phi}\dot{\delta}_m = 0, \quad (85)$$

$$\ddot{\delta}_m + \left(2H - Q\frac{\dot{\phi}}{M_{\rm pl}}\right)\dot{\delta}_m - \frac{\rho_m^*\delta_m}{2M_{\rm pl}^2}(1 - 2Q^2) + \left[\frac{V_{,\phi}}{M_{\rm pl}^2} + \frac{Q}{M_{\rm pl}}\left(m_\phi^2 + \frac{2k^2}{a^2} - 6H^2 - 6\dot{H} - \frac{2\dot{\phi}^2}{M_{\rm pl}^2} - 2Q\frac{V_{,\phi}}{M_{\rm pl}} - 2Q^2\frac{\rho_m^*}{M_{\rm pl}^2}\right)\right]\delta\phi + \frac{1}{M_{\rm pl}} \times \left(2Q^2\frac{\dot{\phi}}{M_{\rm pl}} - \frac{2\dot{\phi}}{M_{\rm pl}} - 2QH\right)\delta\dot{\phi} = 0, \quad (86)$$

where $m_\phi^2 = V_{,\phi\phi}$ is the mass squared of the chameleon field.

As long as the field ϕ evolves slowly ("adiabatically") along the instantaneous minima of the effective potential $V_{\rm eff}$, one can employ the quasistatic approximation on subhorizon scales ($k \gg aH$) [65,66,69]. This corresponds to the approximation under which the dominant terms in Eqs. (85) and (86) are those including k^2/a^2, m_ϕ, and δ_m, i.e.,

$$\left(m_\phi^2 + \frac{k^2}{a^2}\right)\delta\phi \simeq -\frac{Q}{M_{\rm pl}}\rho_m^*\delta_m, \quad (87)$$

$$\ddot{\delta}_m + 2H\dot{\delta}_m - \frac{\rho_m^*\delta_m}{2M_{\rm pl}^2}(1 - 2Q^2) + \frac{Q}{M_{\rm pl}}\left(m_\phi^2 + \frac{2k^2}{a^2}\right)\delta\phi \simeq 0, \quad (88)$$

where we have also used the approximation $\dot{\phi}/M_{\rm pl} \ll H$. Combining these equations, it follows that

$$\ddot{\delta}_m + 2H\dot{\delta}_m - 4\pi G_{\rm eff}\rho_m^*\delta_m \simeq 0, \quad (89)$$

where the effective gravitational coupling is given by

$$G_{\rm eff} = G\left(1 + 2Q^2\frac{k^2/a^2}{m_\phi^2 + k^2/a^2}\right). \quad (90)$$

An analogous modified equation was found in Refs. [11,66,70], the crucial point being to elucidate the physical significance of $G_{\rm eff}$. We can understand the physical content of the modification of gravity by looking at the corresponding gravitational potential in real space. The gravitational potential (per unit mass) is of the type $V(r) = -(G/r)(1 + 2Q^2e^{-m_\phi r})$ [71].

When we solve the full system of perturbations (86), we can, for some of our models, get a small discrepancy compared to (89). This can result in a non-negligible difference of up to around 5% in the numerical calculation of the growth rate of matter perturbations. This arises mainly because the field ϕ does not move exactly along the minimum of the effective potential but is instead lagging a little behind it.

We see that in chameleon models $G_{\rm eff}$ is a scale-dependent as well as a time-dependent quantity. Clearly the scale-dependent driving force in Eq. (90) induces in turn a scale dependence in the growth of matter perturbations with two asymptotic regimes, i.e.,

$$G_{\rm eff} = G(1 + 2Q^2) \qquad k/a \gg m_\phi \quad \text{or} \quad \lambda \ll \lambda_c \quad (91)$$

$$G_{\rm eff} = G \qquad k/a \ll m_\phi \quad \text{or} \quad \lambda \gg \lambda_c, \quad (92)$$

where we have introduced the physical wavelength $\lambda = (2\pi/k)a$. We have in particular $\lambda_0 = 2\pi/k$ today ($a = 1$). The characteristic (physical) scale λ_c is defined by

$$\lambda_c = 2\pi/m_\phi. \quad (93)$$

On scales $\lambda \gg \lambda_c$ matter perturbations do not feel the fifth force during their growth. On the contrary, on scales much smaller than λ_c they do feel its presence. During the matter dominance ($\Omega_m^* \simeq 1$) the solutions to Eq. (89) are given by

$$\delta_m \propto a^{[\sqrt{1+24(1+2Q^2)}-1]/4} \qquad \lambda \ll \lambda_c, \quad (94)$$

$$\delta_m \propto a \qquad \lambda \gg \lambda_c. \quad (95)$$

Hence, in the regime $\lambda \ll \lambda_c$, the growth rate gets larger than that in standard general relativity.

As mentioned earlier, a powerful way to describe the growth of perturbations is by introducing the function $\gamma(k, z)$ defined as follows:

$$f = \Omega_m^*(z)^{\gamma(k,z)}, \quad (96)$$

where

$$f = \frac{d\ln\delta_m}{d\ln a}. \tag{97}$$

Remember the definition $\delta_m \equiv \delta\rho_m^*/\rho_m^*$. The quantity γ can be time-dependent and also scale-dependent. It is known that a large class of dark energy models inside general relativity yields a quasiconstant γ with values close to that of the ΛCDM model, $\gamma \approx 0.55$ [45,46]. Therefore any significant deviation from this behavior would give rise to a characteristic signature for our chameleon models. Since $0 < \Omega_m^*(z) < 1$, smaller γ implies a larger growth rate of matter perturbations.

As we have seen before, the chameleon mechanism is devised so that in high-density environments the mass of the scalar field is large relative to its value in low-density ones. During the cosmological evolution, the mass of the field will follow this behavior, which means that λ_c will move from small to large values. In other words, $G_{\rm eff}$ will evolve from the regime (92) to the regime (91). This transition is scale-dependent, which is an important feature of the growth of matter perturbations in chameleon [and $f(R)$] models.

We consider the evolution of matter perturbations for the wave numbers

$$0.01h\ \mathrm{Mpc}^{-1} \lesssim k \lesssim 0.2h\ \mathrm{Mpc}^{-1}, \tag{98}$$

where h describes the uncertainty of the Hubble parameter H_0 today, i.e. $H_0 = 100h\ \mathrm{km\,sec^{-1}\,Mpc^{-1}}$. The scales (98) range from the upper limit of observable scales in the linear regime of perturbations to the mildly nonlinear regime (in which the linear approximation is still reasonable).

Depending on the value of λ_c today (denoted as $\lambda_{c,0}$) and on its recent evolution, three possibilities can actually arise: (i) The model is hardly distinguishable from ΛCDM. (ii) The model is distinguishable from ΛCDM but shows no dispersion, i.e., no scale dependence. In this case low values of γ_0 will also yield large slopes $\gamma_0' \equiv (d\gamma/dz)(z=0)$, much larger than in ΛCDM. (iii) The model is distinguishable from ΛCDM and shows some dispersion altogether. These three cases can be characterized using the quantity $\gamma_0 \equiv \gamma(z=0)$. This classification is analogous to what was done for some viable $f(R)$ models [54] and it can be defined as follows:

(i) The region in parameter space for which $\gamma_0 > 0.53$ for all the scales described by (98). In this region γ_0' is small and γ is nearly constant.
The region where γ_0 is degenerate, i.e., assumes the same value for all the scales, with a value smaller than 0.5. In this region γ_0' is large and there is a significant variation of γ.

(ii) The region where γ_0 shows some dispersion, i.e., a scale dependence. For low γ_0, γ_0' is large and we have significant changes of γ.

Models in the regions (ii) and (iii) can be clearly discriminated from ΛCDM. Some examples are shown in Figs. 6 and 7. We investigate below in more detail the appearance of these characteristic signatures.

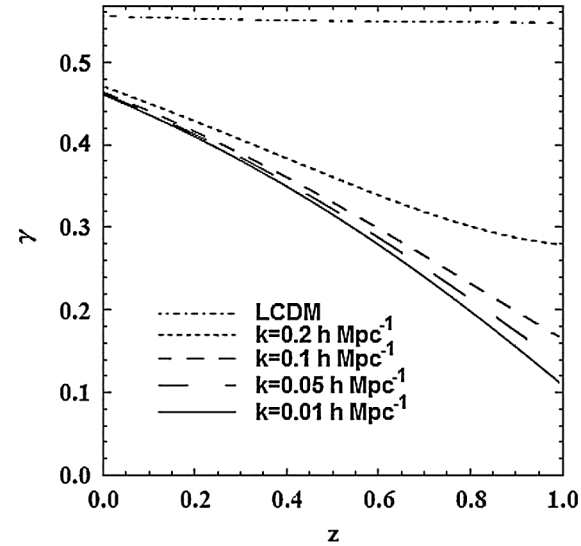

FIG. 6. The evolution of the growth index $\gamma(z)$ versus the redshift z in the model (58) with $n = 0.8$, $\mu = 0.5$, and $Q = 1/\sqrt{6}$ for four different values of k. For these parameters, the model passes local gravity constraints. In this case the field is lagging behind the minimum, which means that the approximated equation (89) provides the results slightly different from this plot (by around 4% in the value of γ_0).

B. Observational signatures in the growth of matter perturbations

The main question when looking at linear perturbations in chameleon models is the order of magnitude of the scale λ_c. If the chameleon mass m_ϕ is large such that λ_c is less than the order of the galactic size, matter perturbations on the scales relevant to large scale structures do not feel the chameleon's presence. This is actually the case for the inverse-power exponential potential (56) with model parameters bounded by observational and local gravity constraints. Therefore, we will concentrate the analysis of the perturbations on the potential (58).

In the regime $\phi/M_{\rm pl} \ll 1$ one can employ the approximation $V(\phi) \simeq M^4[1 - \mu(\phi/M_{\rm pl})^n]$. In fact this approximation is valid for most of the cosmological evolution by today. Then we obtain the field mass at the minimum of the effective potential $V_{\rm eff}(\phi)$:

$$m_\phi \simeq \frac{2\pi}{\lambda_{c,0}} e^{-(3(2-n)/2(1-n))N}, \tag{99}$$

where $\lambda_{c,0}$ is the critical length today, given by

$$\lambda_{c,0} = \frac{2\pi}{\sqrt{\mu n(1-n)}} \frac{M_{\rm pl}}{M^2} \left(\frac{Q}{\mu n} \frac{\rho_m^{(0)}}{M^4}\right)^{-(2-n)/[2(1-n)]}. \tag{100}$$

Using the relation $\rho_{\rm DE}^{(0)} = 3M_{\rm pl}^2 H_0^2 \Omega_{\rm DE}^{(0)} \simeq M^4$, we find that $\lambda_{c,0}$ is at most of the order of H_0^{-1}. If $Q = 1$, $n = 0.6$,

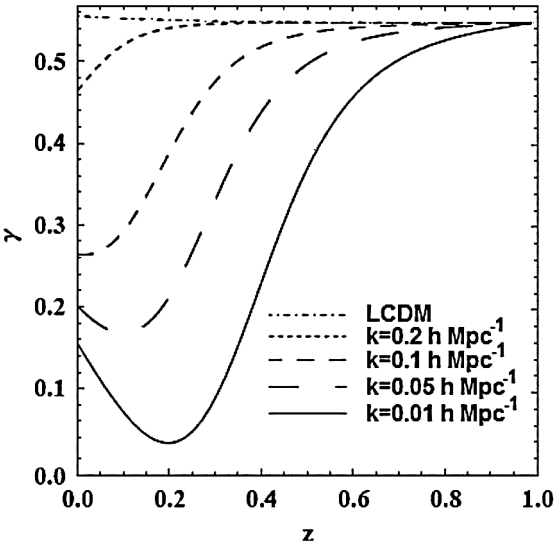

FIG. 7. The evolution of γ versus the redshift z in the model (58) with $n = 0.7$, $\mu = 0.05$, and $Q = 1$ for four different values of k. In this case the model passes local gravity constraints, too. Contrary to Fig. 6 we have a significant dispersion of γ, depending on the wave numbers k.

$\mu = 0.05$, and $\Omega_{\rm DE}^{(0)} = 0.72$, for example, $\lambda_{c,0} \approx 0.4H_0^{-1}$. For the modes deep inside the Hubble radius today ($\lambda_0 \ll H_0^{-1}$) the perturbations are affected by the modification of gravity.

Plugging Eq. (99) into Eq. (90), the effective gravitational coupling can be expressed in the form

$$G_{\rm eff} = G\left[1 + \frac{2Q^2}{1 + e^{-A(N-N_c)}}\right], \tag{101}$$

where

$$A = \frac{4-n}{1-n}, \tag{102}$$

$$N_c = \frac{2(1-n)}{4-n}\ln\left(\frac{\lambda_0}{\lambda_{c,0}}\right). \tag{103}$$

Here A and N_c are the parameters describing, respectively, the steepness of transition from the inferior to the superior asymptote and the position of the half-amplitude value of the function [i.e., $G_{\rm eff} = G(1 + Q^2)$].

The first interesting point to remark is that the steepness of transition depends exclusively on the value of n, with a step function as a limit when $n \to 1$ and a slower transition for $n \to 0$. Nonetheless, it must be remembered that this is so in the variable N. When converting back to the redshift z, the logarithm scale introduces a distortion, which means that the earlier a scale starts its transition, the slower this transition will be. In this sense, there is a scale dependence to the steepness of the transition, even if it does not appear explicitly in Eq. (102).

If we want to get a better feel for the epoch of the transition, we can define the redshift $z_c = e^{-N_c} - 1$. From Eq. (103) it follows that

$$z_c = \left(\frac{\lambda_{c,0}}{\lambda_0}\right)^{2(1-n)/(4-n)} - 1. \tag{104}$$

As expected, the transition redshift is scale-dependent, with higher values for the smaller scales. Moreover, $z_c \to 0$ for all scales when $n \to 1$. Since this is also the limit at which the transition becomes a step function, we have thus an indication that a transition that happens very close to the present will necessarily be very steep. Another remark is that the transition happens in the past ($z_c > 0$) for the scales λ_0 smaller than $\lambda_{c,0}$. Thus $\lambda_{c,0}$ is a good indication of the scale around which there will be a dispersion, as it marks the scale that will be exactly in the middle of the transition today.

If we write z_c explicitly in terms of the parameters and constants of the model, we obtain

$$z_c = \left[\frac{(\mu n)^{1/(1-n)}}{1-n}\frac{k^2 M_{\rm pl}^2}{M^4}\left(Q\frac{\rho_m^{(0)}}{M^4}\right)^{-(2-n)/(1-n)}\right]^{(1-n)/(4-n)} - 1. \tag{105}$$

This shows that z_c gets larger with increasing μ (as the deviation from the ΛCDM model is more significant) and/or decreasing Q. Although the transition occurs earlier for a weaker coupling Q, we need to take into account the fact that the growth rate in the regime $z < z_c$ is smaller for a weaker coupling.

Let us proceed to the numerical analysis of the growth of perturbations. In Fig. 6 we plot the evolution of the growth indices γ for $Q = 1/\sqrt{6}$, $n = 0.8$, and $\mu = 0.5$ for a number of different wave numbers within the range specified by Eq. (98). Note that these parameters satisfy the local gravity constraints discussed in Sec. V (see Fig. 4). At the present epoch these modes are in the regime (ii), with very similar growth indices today ($\gamma_0 \simeq 0.46$). As estimated by Eq. (105) the transition redshift z_c is larger than the order of 1 for $k \gtrsim 0.05h$ Mpc^{-1}, e.g., $z_c = 2.3$ for $k = 0.1h$ Mpc^{-1}. The degenerate behavior similar to that shown in Fig. 6 has also been found in some $f(R)$ models [48,54]. Numerically we have verified that values of γ_0 in this case are slightly higher than those expected in the asymptotic regime ($\lambda \ll \lambda_c$). This discrepancy comes from the fact that the chameleon field is lagging behind the minimum of the potential for this choice of parameters. As a result, we need to solve the full perturbation equations (85) and (86) instead of the approximated equation (89). Our numerical results show that there can be a discrepancy of up to a few percent in the growth rate calculated with the two different methods.

Another choice of parameters, which are compatible with local gravity constraints, is made in Fig. 7, where we see the evolution of the growth indices γ for $Q = 1$,

$n = 0.7$, and $\mu = 0.05$. The behavior of the growth indices is very different from the one shown in Fig. 6. Clearly this corresponds to the regime (iii), in which γ_0 is dispersed with respect to the wave numbers k. The reason for the dispersion is that the transition to the regime $\lambda \ll \lambda_c$ occurs on lower redshifts than in the case shown in Fig. 6.

In Fig. 8 we illustrate three different regimes in the (n, μ) plane for the couplings $Q = 1/\sqrt{6}$ and $Q = 1$. For the model parameters close to $(n, \mu) = (1, 0)$, the perturbations behave similarly to those in the ΛCDM model [i.e., in the region (i)]. Figure 8 shows that the limits imposed by the constraints derived in Sec. V, although strong, allow the large parameter space for the existence of an enhanced growth of matter perturbations and for the presence of the dispersion of γ_0. Finally we note that the large variation of γ in the regime $z \lesssim 1$ seen in Figs. 6 and 7 will also enable us to distinguish the chameleon models from the ΛCDM model.

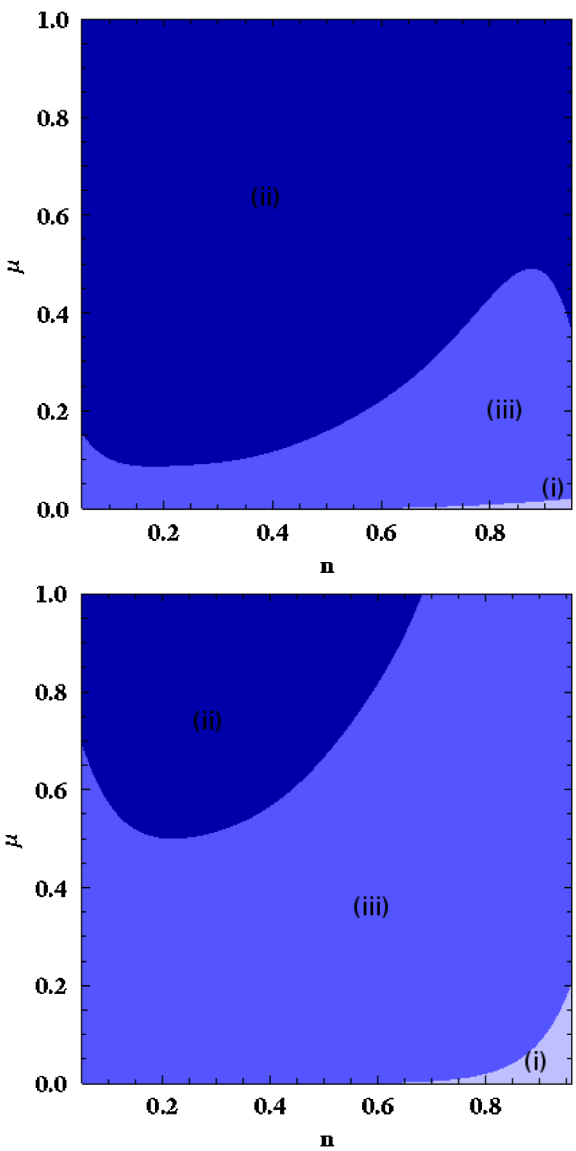

FIG. 8 (color online). The regions (i), (ii), and (iii) in the (n, μ) space for $Q = 1/\sqrt{6}$ (top) and for $Q = 1$ (bottom). In the region (i) all the modes have $\gamma_0 > 0.53$. In region (ii) γ_0 is degenerate with the value smaller than 0.5, and (iii) shows the regime where γ_0 is dispersed. It is clear that, for both choices of Q, there are viable choices of parameters in which the deviation from the ΛCDM model is present.

VII. SUMMARY AND CONCLUSIONS

In this paper we have studied observational signatures of a chameleon scalar field coupled to nonrelativistic matter. If the chameleon field is responsible for the late-time cosmic acceleration, the field potentials need to be consistent with the small energy scale of dark energy as well as local gravity constraints. We showed that the inverse-power potential cannot satisfy both cosmological and local gravity constraints. In general, we require that the chameleon potentials are of the form $V(\phi) = M^4[1 + f(\phi)]$, where the function $f(\phi)$ is smaller than 1 today and M is a mass that corresponds to the dark energy scale ($M \sim 10^{-12}$ GeV).

The potential $V(\phi) = M^4 \exp[\mu(M/\phi)^n]$ is one of those viable candidates. However, we showed that the allowed model parameter space is tightly constrained by the 2006 Eöt-Wash experiment. As we see in Fig. 3, the natural parameters with n and Q of the order of unity are excluded for $\mu = 1$. Unless we choose unnatural values of μ smaller than 10^{-5}, this potential is incompatible with local gravity constraints for $\{n, Q\} = \mathcal{O}(1)$.

On the other hand, the chameleon potential $V(\phi) = M^4[1 - \mu(1 - e^{-\phi/M_{\rm pl}})^n]$, which has the asymptotic form $V(\phi) \simeq M^4[1 - \mu(\phi/M_{\rm pl})^n]$ in the regime $\phi \ll M_{\rm pl}$, can be consistent with a number of local gravity experiments as well as cosmological constraints. In fact this case covers the viable potentials of $f(R)$ dark energy models in the Einstein frame. The allowed parameter regions in the (n, Q) plane are illustrated in Figs. 4 and 5 for $\mu = 0.5$ and $\mu = 0.05$. This potential is viable for $n > 0.6$ and for the coupling Q of the order of unity.

In order to distinguish the chameleon models from the ΛCDM model at the background level, we discussed the evolution of the statefinders (r, s) defined in Eq. (63). Unlike the ΛCDM model in which r and s are constant ($r = 1$, $s = 0$) the statefinders exhibit a peculiar evolution, as plotted in Fig. 2. For the potential $V(\phi) = M^4[1 - \mu(1 - e^{-\phi/M_{\rm pl}})^n]$ we found that $r < 1$ and $s > 0$ around the present epoch, but the solutions approach the de Sitter point $(r, s) = (1, 0)$ in future. The upcoming observations of SN Ia may discriminate such an evolution from other dark energy models.

We have also studied the growth of matter perturbations for the chameleon potential $V(\phi) = M^4[1 - \mu(1 - e^{-\phi/M_{\rm pl}})^n]$. The presence of a fifth force between the field and nonrelativistic matter (dark matter/baryons) modifies the equation of matter perturbations, provided that the field

mass m_ϕ is smaller than the physical wave number k/a, or $\lambda < \lambda_c$. Cosmologically the field is heavy in the past (i.e., for large density), but the mass m_ϕ decreases by today (typically of the order of H_0) in order to realize the late-time cosmic acceleration. Then the transition from the regime $k/a < m_\phi$ ($\lambda > \lambda_c$) to the regime $k/a > m_\phi$ ($\lambda < \lambda_c$) can occur at the redshift z_c given in Eq. (105). For the perturbations on smaller scales (i.e., larger k) the critical redshift z_c tends to be larger.

For the model parameters and the coupling Q bounded by a number of experimental and cosmological constraints, we have studied the evolution of the growth index γ of matter perturbations. Apart from the "general relativistic regime" in which two parameters n and μ of the potential (58) are close to $(n, \mu) = (1, 0)$, we found that the values of γ today exhibit either dispersion with respect to the wave numbers k [region (iii) in Fig. 8] or no dispersion, however with γ_0 smaller than 0.5 [region (ii) in Fig. 8]. Both cases can be distinguished from the ΛCDM model (where $\gamma \simeq 0.55$). Moreover, as seen in Figs. 6 and 7, the variation of γ on low redshifts is significant.

From observations of galaxy clustering we have not yet obtained the accurate evolution of γ. This is linked to the fact that all probes of clustering are plagued by a bias problem. However upcoming galaxy surveys may pin down the matter power spectrum to exquisite accuracy, together with a better understanding of bias. In order to confirm or rule out models like ours, one must also address the observability of γ both as a function of z and k. We hope that future observations will provide an exciting possibility to detect the fifth force induced by the chameleon scalar field.

ACKNOWLEDGMENTS

D. P. thanks JSPS for financial support during his stay at Tokyo University of Science. D. F. M. and H. A. W. thank the Research Council of Norway FRINAT Grant No. 197251/V30. D. F. M. is also partially supported by Projects No. CERN/FP/109381/2009 and No. PTDC/FIS/102742/2008. B. M. thanks Research Council of Norway (Yggdrasil Program Grant No. 202629V11) for financial support during his stay at the University of Oslo where part of this work was carried out and thanks D. F. M. and H. A. W. for the hospitality. R. G. thanks CTP, Jamia Millia Islamia, for hospitality where a part of this work was carried out. The work of S. T. was supported by the Grant-in-Aid for Scientific Research Fund of the JSPS No. 30318802 and by the Grant-in-Aid for Scientific Research on Innovative Areas (No. 21111006). S. T. thanks Savvas Nesseris, Kazuya Koyama, Burin Gumjudpai, and Jungjai Lee for warm hospitality during his stays in the Niels Bohr Institute, the University of Portsmouth, Naresuan University, and Daejeon.

[1] V. Sahni and A. A. Starobinsky, Int. J. Mod. Phys. D **9**, 373 (2000); S. M. Carroll, Living Rev. Relativity **4**, 1 (2001); T. Padmanabhan, Phys. Rep. **380**, 235 (2003); P. J. E. Peebles and B. Ratra, Rev. Mod. Phys. **75**, 559 (2003); E. J. Copeland, M. Sami, and S. Tsujikawa, Int. J. Mod. Phys. D **15**, 1753 (2006); A. De Felice and S. Tsujikawa, Living Rev. Relativity **13**, 3 (2010); P. Brax, arXiv:0912.3610; S. Tsujikawa, arXiv:1004.1493.
[2] S. Weinberg, Rev. Mod. Phys. **61**, 1 (1989).
[3] Y. Fujii, Phys. Rev. D **26**, 2580 (1982); L. H. Ford, Phys. Rev. D **35**, 2339 (1987); C. Wetterich, Nucl. Phys. **B302**, 668 (1988); B. Ratra and J. Peebles, Phys. Rev. D **37**, 3406 (1988); T. Chiba, N. Sugiyama, and T. Nakamura, Mon. Not. R. Astron. Soc. **289**, L5 (1997); R. R. Caldwell, R. Dave, and P. J. Steinhardt, Phys. Rev. Lett. **80**, 1582 (1998).
[4] S. M. Carroll, Phys. Rev. Lett. **81**, 3067 (1998).
[5] M. Gasperini and G. Veneziano, Phys. Rep. **373**, 1 (2003).
[6] M. Gasperini, F. Piazza, and G. Veneziano, Phys. Rev. D **65**, 023508 (2001); T. Damour, F. Piazza, and G. Veneziano, Phys. Rev. Lett. **89**, 081601 (2002).
[7] J. Khoury and A. Weltman, Phys. Rev. Lett. **93**, 171104 (2004).
[8] J. Khoury and A. Weltman, Phys. Rev. D **69**, 044026 (2004).
[9] I. Navarro and K. Van Acoleyen, J. Cosmol. Astropart. Phys. 02 (2007) 022; T. Faulkner, M. Tegmark, E. F. Bunn, and Y. Mao, Phys. Rev. D **76**, 063505 (2007).
[10] S. Capozziello and S. Tsujikawa, Phys. Rev. D **77**, 107501 (2008).
[11] S. Tsujikawa, K. Uddin, S. Mizuno, R. Tavakol, and J. Yokoyama, Phys. Rev. D **77**, 103009 (2008).
[12] L. Amendola, R. Gannouji, D. Polarski, and S. Tsujikawa, Phys. Rev. D **75**, 083504 (2007); B. Li and J. D. Barrow, Phys. Rev. D **75**, 084010 (2007); L. Amendola and S. Tsujikawa, Phys. Lett. B **660**, 125 (2008); W. Hu and I. Sawicki, Phys. Rev. D **76**, 064004 (2007); A. A. Starobinsky, JETP Lett. **86**, 157 (2007); S. A. Appleby and R. A. Battye, Phys. Lett. B **654**, 7 (2007); S. Tsujikawa, Phys. Rev. D **77**, 023507 (2008); E. V. Linder, Phys. Rev. D **80**, 123528 (2009).
[13] A. A. Starobinsky, Phys. Lett. **91B**, 99 (1980).
[14] L. Amendola, Phys. Rev. D **62**, 043511 (2000).
[15] P. Brax, C. van de Bruck, A. C. Davis, J. Khoury, and A. Weltman, Phys. Rev. D **70**, 123518 (2004).
[16] D. F. Mota and J. D. Barrow, Phys. Lett. B **581**, 141 (2004).
[17] D. F. Mota and D. J. Shaw, Phys. Rev. Lett. **97**, 151102 (2006).
[18] P. Brax, C. van de Bruck, A. C. Davis, and A. M. Green, Phys. Lett. B **633**, 441 (2006).

[19] B. Feldman and A. E. Nelson, J. High Energy Phys. 08 (2006) 002.
[20] D. F. Mota and D. J. Shaw, Phys. Rev. D **75**, 063501 (2007).
[21] P. Brax, C. van de Bruck, A. C. Davis, D. F. Mota, and D. J. Shaw, Phys. Rev. D **76**, 085010 (2007).
[22] P. Brax, C. van de Bruck, and A. C. Davis, Phys. Rev. Lett. **99**, 121103 (2007).
[23] P. Brax and J. Martin, Phys. Lett. B **647**, 320 (2007).
[24] P. Brax, C. van de Bruck, A. C. Davis, D. F. Mota, and D. J. Shaw, Phys. Rev. D **76**, 124034 (2007).
[25] A. E. Nelson and J. Walsh, Phys. Rev. D **77**, 095006 (2008).
[26] T. Tamaki and S. Tsujikawa, Phys. Rev. D **78**, 084028 (2008).
[27] P. Brax, C. van de Bruck, A. C. Davis, and D. J. Shaw, Phys. Rev. D **78**, 104021 (2008).
[28] H. Gies, D. F. Mota, and D. J. Shaw, Phys. Rev. D **77**, 025016 (2008).
[29] D. F. Mota, V. Pettorino, G. Robbers, and C. Wetterich, Phys. Lett. B **663**, 160 (2008).
[30] A. C. Davis, C. A. O. Schelpe, and D. J. Shaw, Phys. Rev. D **80**, 064016 (2009).
[31] A. S. Chou *et al.* (GammeV Collaboration), Phys. Rev. Lett. **102**, 030402 (2009).
[32] S. Tsujikawa, T. Tamaki, and R. Tavakol, J. Cosmol. Astropart. Phys. 05 (2009) 020.
[33] I. Thongkool, M. Sami, R. Gannouji, and S. Jhingan, Phys. Rev. D **80**, 043523 (2009).
[34] P. Brax, C. Burrage, A. C. Davis, D. Seery, and A. Weltman, Phys. Rev. D **81**, 103524 (2010).
[35] A. Upadhye, J. H. Steffen, and A. Weltman, Phys. Rev. D **81**, 015013 (2010).
[36] P. Brax, C. van de Bruck, A. C. Davis, D. J. Shaw, and D. Iannuzzi, Phys. Rev. Lett. **104**, 241101 (2010).
[37] P. Brax, R. Rosenfeld, and D. A. Steer, J. Cosmol. Astropart. Phys. 08 (2010) 033.
[38] P. Brax, C. van de Bruck, D. F. Mota, N. J. Nunes, and H. A. Winther, Phys. Rev. D **82**, 083503 (2010).
[39] D. J. Kapner *et al.*, Phys. Rev. Lett. **98**, 021101 (2007).
[40] For a review of experimental tests of the equivalence principle and general relativity, see C. M. Will, *Theory and Experiment in Gravitational Physics*, 2nd ed. (Basic Books/Perseus Group, New York, 1993); Living Rev. Relativity **9**, 3 (2005).
[41] R. Nagata, T. Chiba, and N. Sugiyama, Phys. Rev. D **69**, 083512 (2004).
[42] V. Sahni, T. D. Saini, A. A. Starobinsky, and U. Alam, JETP Lett. **77**, 201 (2003).
[43] U. Alam, V. Sahni, T. D. Saini, and A. A. Starobinsky, Mon. Not. R. Astron. Soc. **344**, 1057 (2003).
[44] L. M. Wang and P. J. Steinhardt, Astrophys. J. **508**, 483 (1998).
[45] E. V. Linder, Phys. Rev. D **72**, 043529 (2005).
[46] D. Polarski and R. Gannouji, Phys. Lett. B **660**, 439 (2008).
[47] R. Gannouji and D. Polarski, J. Cosmol. Astropart. Phys. 05 (2008) 018.
[48] R. Gannouji, B. Moraes, and D. Polarski, J. Cosmol. Astropart. Phys. 02 (2009) 034.
[49] H. Motohashi, A. A. Starobinsky, and J. Yokoyama, Prog. Theor. Phys. **123**, 887 (2010).
[50] T. Narikawa and K. Yamamoto, Phys. Rev. D **81**, 043528 (2010).
[51] U. Alam, V. Sahni, and A. A. Starobinsky, Astrophys. J. **704**, 1086 (2009).
[52] J. H. He, B. Wang, and Y. P. Jing, J. Cosmol. Astropart. Phys. 07 (2009) 030.
[53] R. Gannouji, B. Moraes, and D. Polarski, arXiv:0907.0393.
[54] S. Tsujikawa, R. Gannouji, B. Moraes, and D. Polarski, Phys. Rev. D **80**, 084044 (2009).
[55] R. Bean and M. Tangmatitham, Phys. Rev. D **81**, 083534 (2010).
[56] A. Cimatti *et al.*, arXiv:0912.0914.
[57] R. Gannouji, D. Polarski, A. Ranquet, and A. A. Starobinsky, J. Cosmol. Astropart. Phys. 09 (2006) 016.
[58] L. Amendola, M. Kunz, and D. Sapone, J. Cosmol. Astropart. Phys. 04 (2008) 013; C. Di Porto and L. Amendola, Phys. Rev. D **77**, 083508 (2008).
[59] D. F. Mota, J. R. Kristiansen, T. Koivisto, and N. E. Groeneboom, Mon. Not. R. Astron. Soc. **382**, 793 (2007); T. Koivisto and D. F. Mota, J. Cosmol. Astropart. Phys. 06 (2008) 018.
[60] S. Nesseris and L. Perivolaropoulos, Phys. Rev. D **77**, 023504 (2008).
[61] L. Knox, Y. S. Song, and J. A. Tyson, Phys. Rev. D **74**, 023512 (2006); Y. S. Song and K. Koyama, J. Cosmol. Astropart. Phys. 01 (2009) 048; Y. S. Song and O. Dore, J. Cosmol. Astropart. Phys. 03 (2009) 025.
[62] D. F. Mota, D. J. Shaw, and J. Silk, Astrophys. J. **675**, 29 (2008); D. F. Mota, J. Cosmol. Astropart. Phys. 09 (2008) 006.
[63] G. Esposito-Farèse and D. Polarski, Phys. Rev. D **63**, 063504 (2001).
[64] J. M. Bardeen, Phys. Rev. D **22**, 1882 (1980).
[65] A. A. Starobinsky, JETP Lett. **68**, 757 (1998).
[66] B. Boisseau, G. Esposito-Farese, D. Polarski, and A. A. Starobinsky, Phys. Rev. Lett. **85**, 2236 (2000).
[67] J. c. Hwang, Astrophys. J. **375**, 443 (1991).
[68] L. Amendola, Mon. Not. R. Astron. Soc. **312**, 521 (2000); Phys. Rev. D **69**, 103524 (2004); L. Amendola, S. Tsujikawa, and M. Sami, Phys. Lett. B **632**, 155 (2006).
[69] S. Tsujikawa, Phys. Rev. D **76**, 023514 (2007); S. Tsujikawa, K. Uddin, and R. Tavakol, Phys. Rev. D **77**, 043007 (2008); A. De Felice, S. Mukohyama, and S. Tsujikawa, Phys. Rev. D **82**, 023524 (2010).
[70] Y. S. Song, L. Hollenstein, G. Caldera-Cabral, and K. Koyama, J. Cosmol. Astropart. Phys. 04 (2010) 018.
[71] L. Amendola and S. Tsujikawa, *Dark Energy—Theory and Observations* (Cambridge University Press, Cambridge, England, 2010.